A Conducting Sheet Model for Efficient Wide Band FDTD Analysis of Planar Waveguides and Circuits

A. Lauer and I. Wolff
Institute of Mobile and Satellite Communication Techniques,
D–47475 Kamp-Lintfort, Germany, e-mail lauer@imst.de

Abstract—**A simple wide band equivalent circuit for the surface impedance of conducting sheets is introduced into the three dimensional Yee FDTD scheme. The model is based on the plane skin effect, thus the frequency dependence of losses and of the inner inductivity is included. Stability considerations are presented as well as numerical results for the attenuation coefficient of microstrip and coplanar waveguides in comparison to reference data.**

I. Introduction

Metallic losses in microwave waveguides and circuits cannot be treated efficiently using straight forward FDTD simulations, since the skin effect is much smaller and faster than the wave propagation itself. Thus the simulation time would be increased by magnitudes.

Therefore thin conducting sheet approximations have been introduced into the Yee [1] FDTD scheme, which work well in mono-frequent and narrow band applications [2]–[4].

This contribution presents a conducting sheet approximation suitable for wide band FDTD simulations, which properly models losses as well as the inner inductivity under assumption of the plane skin effect.

In section II a simple approximative wide band equivalent circuit consisting of two inductors and three resistors is proposed for modeling the sheet's surface impedance.

Section III shows how this circuit is introduced into Yee's FDTD scheme, yielding the need of only two additional nodes[1] per tangential electric node on the conducting sheet. Stability considerations follow in section IV.

Numerical results for the attenuation coefficient of microstrip and coplanar waveguides are given in section V and compared to those of measurements, static two dimensional FD calculations [5] and an approximate formula for MSL ohmic losses [6].

II. A Simple Equivalent Circuit for the Surface Impedance of Thin Conducting Sheets

Assuming a plane skin effect, the surface admittance Y_s (rsp. the admittance of a square part of the sheet $Y_\Box$) can be written as

$$
\begin{aligned}
Y_\Box &= 2Y_\mathrm{s} = 2\frac{H_\mathrm{s}}{E_\mathrm{s}} = G_{0,\Box}\frac{\tanh((1+\mathrm{j})\sqrt{\Omega})}{(1+\mathrm{j})\sqrt{\Omega}},\\
\Omega &= \frac{\omega}{\omega_0}, \quad \omega_0 = \frac{8}{\mu\sigma t^2}, \quad G_{0,\Box} = \frac{1}{R_{0,\Box}} = \kappa t.
\end{aligned} \tag{1}
$$

Herein t is the sheet's thickness and σ is its conductivity.

A second order rational approximation[2] for *real value* arguments x yields

$$
\begin{aligned}
f(x) &= \frac{\tanh\sqrt{x}}{\sqrt{x}} \approx \\
h(x) &= \frac{0.00037835\,x^2 + 0.089376\,x + 0.999241}{0.00936184\,x^2 + 0.419520\,x + 1},
\end{aligned} \tag{2}
$$

the approximation interval was $[0,80]$, the maximum relative error was estimated to be 0.076%.

For the needed *complex*[3] $x = (1+\mathrm{j})^2\Omega$, the relative error $|f(x) - h(x)|/|f(x)|$ is less than 3 % for $\Omega < 10$, less than 6 % for $\Omega < 30$ and less than 10 % for $\Omega < 50$.

Figure 1 shows an equivalent circuit proposed to realize $Y_\Box \approx Y_1 = G_{0,\Box}\,h(\Omega)$. As seen in section III, this circuit can be easily introduced into the Yee scheme.

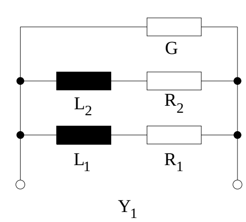

Fig. 1. Equivalent Circuit for the second order rational surface admittance approximation $2Y_\mathrm{s} = Y_\Box \approx Y_1$.

A formulation, that does not depend on the sheet's parameters κ and t, is

$$
h((1+\mathrm{j})^2\Omega) = g + \frac{1}{r_1 + \mathrm{j}\Omega l_1} + \frac{1}{r_2 + \mathrm{j}\Omega l_2}, \tag{3}
$$

with dimensionless

$$
l_i = G_{0,\Box}\,\omega_0 L_i, \quad r_i = G_{0,\Box} R_i, \quad g = \frac{G}{G_{0,\Box}}, \qquad i \in \{1,2\}. \tag{4}
$$

[1]Corresponding to the currents in the two inductors of the equivalent circuit.

[2]Obtained using the "minimax" module of the "numapprox" package in the symbolic algebra program MAPLE V(TM). Optimization criterion was minimization of the maximum relative error.

[3]For a 2 μm thick Au sheet $\omega_0/(2\pi)$ is approx. 6 GHz, yielding $\Omega < 10$ up to a frequency of 60 GHz.

Equation (3) can be solved analytically, resulting in

$$\begin{aligned} r_1 &= 7.482301652, \quad & r_2 &= 1.211859662, \\ l_1 &= 0.353893318, \quad & l_2 &= 0.959481195, \\ g &= 0.040414818. \end{aligned} \tag{5}$$

III. FDTD implementation of the Equivalent Circuit

To obtain an equivalent circuit for the FDTD method itself, the Yee scheme for inhomogeneous material with electric and magnetic losses can be written in a short operator formulation [7], [8].

Figure 2 shows the unit cell of the well known Yee FDTD scheme. Field components as well as the cell sizes and the material properties are functions of the discrete position $X = (i, j, k)^{\mathrm{T}}$. Field components and other properties belonging to the cell X are shown in the figure. For simpler writing, component and direction indices are numbered in a modulo three sense, e. g. $E_0 \equiv E_{\mathrm{x}}$, $E_1 \equiv E_{\mathrm{y}}$, $E_2 \equiv E_{\mathrm{z}}$ and again $E_3 \equiv E_{\mathrm{x}}$ and $E_{-1} \equiv E_{\mathrm{z}}$. Upper indices E rsp. H are used for the electric rsp. magnetic conductivity σ^{E} rsp. σ^{H} and for the sub cell sizes Δ^{E} and Δ^{H}. A lower index "+" means $\nu+1$, a "-" stands for $\nu-1$. The shift operators ξ_ν and $\widehat{\xi}_\nu$ are defined by $\xi_\nu H_\mu(X) = H_\mu(X + \mathcal{E}_\nu)$ and $\widehat{\xi}_\nu H_\mu(X) = H_\mu(X - \mathcal{E}_\nu)$, with the unit vector in ν–direction $\mathcal{E}_\nu$.

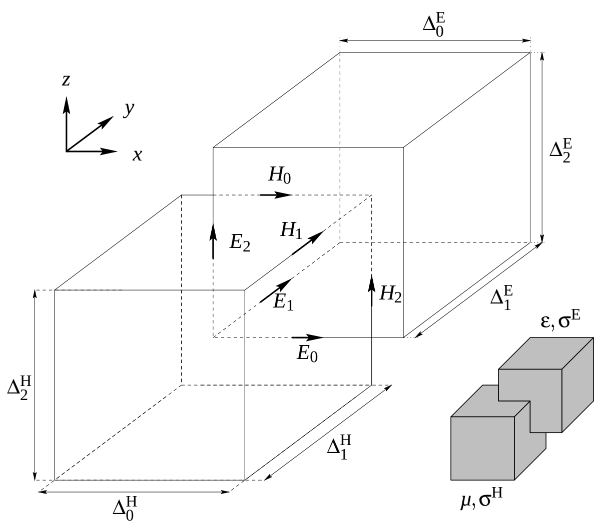

Fig. 2. Yee cell at the position X with the field components and parameters accounted to this cell.

The time continuous Yee scheme for lossy material and graded mesh discretization is

$$\begin{aligned} (\varepsilon_\nu \partial_t + \sigma_\nu^{\mathrm{E}}) E_\nu &= \frac{1}{\Delta_+^{\mathrm{H}}} (\xi_+ - 1) H_- - \frac{1}{\Delta_-^{\mathrm{H}}} (\xi_- - 1) H_+, \\ (\mu_\nu \partial_t + \sigma_\nu^{\mathrm{H}}) H_\nu &= \frac{1}{\Delta_+^{\mathrm{E}}} (\widehat{\xi}_+ - 1) E_- - \frac{1}{\Delta_-^{\mathrm{E}}} (\widehat{\xi}_- - 1) E_+ \end{aligned} \tag{6}$$

with

$$\begin{aligned} \varepsilon_\nu &= \frac{1}{4} \left(1 + \widehat{\xi}_+ + \widehat{\xi}_- + \widehat{\xi}_- \widehat{\xi}_+ \right) \varepsilon, \\ \sigma_\nu^{\mathrm{E}} &= \frac{1}{4} \left(1 + \widehat{\xi}_+ + \widehat{\xi}_- + \widehat{\xi}_- \widehat{\xi}_+ \right) \sigma^{\mathrm{E}}, \\ \mu_\nu &= \frac{1}{4} (1 + \xi_+ + \xi_- + \xi_- \xi_+) \mu, \\ \sigma_\nu^{\mathrm{H}} &= \frac{1}{4} (1 + \xi_+ + \xi_- + \xi_- \xi_+) \sigma^{\mathrm{H}}. \end{aligned} \tag{7}$$

An equivalent circuit formulation for (6) is proposed in [7]. A more general formulation, suitable for graded mesh FDTD schemes, requires magnetic and electric voltages to be introduced to maintain symmetry of the equivalent circuit. With $\Theta_\nu^{\mathrm{E}} = E_\nu \Delta_\nu^{\mathrm{E}}$ and $\Theta_\nu^{\mathrm{H}} = H_\nu \Delta_\nu^{\mathrm{H}}$ equation (6) yields

$$\begin{aligned} (C_\nu \partial_t + G_\nu) \Theta_\nu^{\mathrm{E}} &= (\xi_+ - 1) \Theta_-^{\mathrm{H}} - (\xi_- - 1) \Theta_+^{\mathrm{H}}, \\ (L_\nu \partial_t + R_\nu) \Theta_\nu^{\mathrm{H}} &= (\widehat{\xi}_+ - 1) \Theta_-^{\mathrm{E}} - (\widehat{\xi}_- - 1) \Theta_+^{\mathrm{E}}, \end{aligned} \tag{8}$$

with

$$\begin{aligned} C_\nu &= \frac{\Delta_+^{\mathrm{H}} \Delta_-^{\mathrm{H}}}{\Delta_\nu^{\mathrm{E}}} \varepsilon_\nu, \quad & G_\nu &= \frac{\Delta_+^{\mathrm{H}} \Delta_-^{\mathrm{H}}}{\Delta_\nu^{\mathrm{E}}} \sigma_\nu^{\mathrm{E}}, \\ L_\nu &= \frac{\Delta_+^{\mathrm{E}} \Delta_-^{\mathrm{E}}}{\Delta_\nu^{\mathrm{H}}} \mu_\nu, \quad & R_\nu &= \frac{\Delta_+^{\mathrm{E}} \Delta_-^{\mathrm{E}}}{\Delta_\nu^{\mathrm{H}}} \sigma_\nu^{\mathrm{H}}. \end{aligned} \tag{9}$$

Figure 3 shows an electrical field node of the equivalent circuit belonging to (8).[4] To implement the conducting sheet approximation, all electrical nodes belonging to tangential field components in the conductor are modified as shown in figure 4.

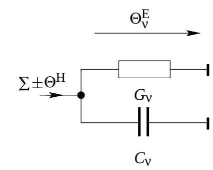

Fig. 3. Equivalent circuit for an electrical field node in the Yee scheme.

Two additional nodes $\Theta_{\nu,1}$ and $\Theta_{\nu,2}$, which are treated like magnetic nodes in the time stepping scheme, are introduced. The 'parasitic' capacitor C_ν is needed to leave the time stepping algorithm unchanged, its value (discussed in section IV) can be chosen very small, thus it does not disturb the surface admittance approximation.

Since $\Theta_\nu^{\mathrm{E}} = E_\nu \Delta_\nu^{\mathrm{E}}$ and $\Theta_{tan}^{\mathrm{H}} = H \Delta_{tan}^{\mathrm{H}}$ for the tangential magnetic field, the proper parameters to realize the conducting sheet's surface admittance Y_1 are

$$\begin{aligned} G_\nu &= \frac{\Delta_{tan}^{\mathrm{H}}}{\Delta_\nu^{\mathrm{E}}} G_{0,\square}\, g, \\ L_{\nu,1} &= \frac{1}{G_{0,\square}\, \omega_0}\, l_1, \quad R_{\nu,1} = \frac{1}{G_{0,\square}}\, r_1, \\ L_{\nu,2} &= \frac{1}{G_{0,\square}\, \omega_0}\, l_2, \quad R_{\nu,2} = \frac{1}{G_{0,\square}}\, r_2. \end{aligned} \tag{10}$$

[4] The summation of the Θ^{H} can be done using four gyrators in parallel [7], in this case, the Θ^{H}–nodes have the same structure as the Θ^{E}–nodes. An alternative is to use four 1:1 transformers, in this case, Θ^{H} is implemented as a current.

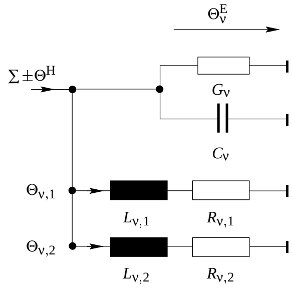

Fig. 4. Modified equivalent circuit for a tangential electrical field node in the conducting sheet.

At the modified nodes, $\Theta_{\mathrm{v},1}$ and $\Theta_{\mathrm{v},2}$ are subtracted from the right side of (8). The newly introduced nodes are treated as

$$\begin{aligned}(L_{\mathrm{v},1}\partial_t + R_{\mathrm{v},1})\,\Theta_{\mathrm{v},1} &= \Theta_\mathrm{v}^\mathrm{E},\\ (L_{\mathrm{v},2}\partial_t + R_{\mathrm{v},2})\,\Theta_{\mathrm{v},2} &= \Theta_\mathrm{v}^\mathrm{E}.\end{aligned} \tag{11}$$

For the discretization in time, one of the well known stepping schemes for lossy FDTD cells can be used.

At the edges of the conducting sheets, G_v has to be halved as well as $L_{\mathrm{v},1}, L_{\mathrm{v},2}$ and $R_{\mathrm{v},1}, R_{\mathrm{v},2}$ are to be doubled for proper operation.

IV. Stability Considerations

As shown in [8] a stability criterion for the unmodified Yee scheme can be written as

$$\left(\frac{1}{\frac{L_\mathrm{v}}{16}C_\mathrm{v}}\right)_{\max} < \frac{4}{\Delta_\mathrm{t}^2}. \tag{12}$$

If the left hand side of (12) is interpreted as an estimate for the maximum angular resonance frequency of the FDTD scheme, an equation for C_v of the modified cells can be obtained,

$$C_\mathrm{v} > \frac{\Delta_\mathrm{t}^2}{4}\left[\left(\frac{16}{L_\mathrm{v}}\right)_{\max} + \frac{1}{L_{\mathrm{v},1}} + \frac{1}{L_{\mathrm{v},2}}\right]. \tag{13}$$

The use of (13) to calculate C_v has two advantages:

1. The time step Δ_t remains unchanged.
2. In practical applications, ωC_v is in the range from 10^{-5} A/V to 10^{-2} A/V, whereas $|Y_\square| > 10$ A/V, e.g. the 'parasitic' capacitor does not influence the accuracy of the simulations.

It is also possible to eliminate the capacitors from the modified nodes, but in this case the time step possibly has to be adjusted to ensure stability.

V. Numerical Validation

For the empirical validation of the approximation, a microstrip and a coplanar waveguide, for which reference data is available, have been simulated to obtain attenuation coefficients.

Both are on a 250 μm Al_2O_3 substrate, the conducting Au ($\sigma = 41$ MA/Vm) films are 5 μm thick. The microstrip line's width is 225 μm, yielding a characteristic impedance of approx. 53.2 Ω. The coplanar waveguide has an inner conductor's width of w = 125 μm, the distance between the inner sides of the outer conductors is d = 225 μm, the characteristic impedance is approx. 48.6 Ω.

A l = 10 mm long part of the waveguides was used for the simulation.

Since a very high accuracy is needed for the simulation of losses < 0.1 dB,

- A Gaussian pulse modulated with a sinus function has been used for excitation in an electric wall. It has been observed, that an unmodulated Gaussian pulse excites small static fields, which disturb the discrete Fourier transform needed for postprocessing.
- Approx. 5 mm and 15 mm away from the exciting wall, the voltages on the transmission lines have been recorded for attenuation calculation.
- No absorbing boundary conditions have been used. The waveguides' total lengths have been chosen big enough, so that the reflected pulse does not disturb the simulation.

The MSL was discretized using 10 cells for both, the conductor's width and the substrate height. The backside metalization was simulated as a conducting sheet, too. The CPW waveguide's inner conductor was discretized using 11 cells, the gap with 5 cells. The substrate was discretized with an eight cell graded mesh.

Figure 5 shows a comparison of the approximative surface admittance Y_1 obtained from voltage and current FDTD results in a microstrip waveguide's backside metalization and the theoretical results from (1). Obviously the conductance as well as the inner inductivity are very accurately modeled in the whole frequency range.

The Figures 6 and 7 compare the simulated attenuation with measurements, static FD results and an approximation for MSL losses. The FDTD results do agree very well with the reference data over the whole frequency range. Radiation losses have not been taken into account in the FDTD simulations.

VI. Conclusions

A wide band FDTD model based on a simple equivalent circuit has been presented for conducting sheet modeling. The sheet's conductance as well as its the inner inductivity, depending on the frequency due to the skin effect, are properly modeled. Excellent results have been obtained simulating lossy microstrip and coplanar waveguides. Because the approximation proposed here has almost no impact on computation time and computer memory consumption, it is suitable for the simulation for most passive planar microwave circuits.

REFERENCES

[1] K. S. Yee, "Numerical solution of initial boundary value problems involving Maxwell's equations in isotropic media," *IEEE Trans. Antennas Propagat.*, vol. AP-14, pp. 302–307, 1966.

[2] J. G. Maloney and G. S. Smith, "The efficient modeling of thin material sheets in the finite-difference time-domain (FDTD) method," *IEEE Trans. Antennas Propagat.*, vol. AP-40, pp. 323–330, 1992.

[3] L.-K. Wu and L.-T. Han, "Implementation and application of resistive sheet boundary condition in the finite-difference time-domain method," *IEEE Trans. Antennas Propagat.*, vol. AP-40, pp. 628–633, 1992.

[4] J. G. Maloney and G. S. Smith, "A comparison of methods for modeling electrically thon dielectric and conducting sheets in the finite–difference time–domain (FDTD) method," *IEEE Trans. Microwave Theory Tech.*, vol. MTT-41, pp. 690–694, 1993.

[5] G. Kibuka, R. Bertenburg, M. Naghed, and I. Wolff, "Coplanar lumped elements and their application in filters on ceramic and gallium arsenide substrates," in *19th European Microwave Conference Proceedings*, pp. 656–661, 1989.

[6] E. Hammerstad and F. Bekkadal, *Microstrip Handbook*, vol. STF 44 A 74169 of *ELAB report*.

[7] I. J. Craddock, C. J. Railton, and J. P. McGeehan, "Derivation and application of a passive equivalent circuit for the Finite Difference Time Domain algorithm," *IEEE Microwave and Guided Wave Lett.*, vol. 6, pp. 40–42, 1996.

[8] A. Lauer and I. Wolff, "Stable and efficient ABCs for graded mesh fdtd simulations," in *IEEE MTT-S Int. Microwave Symp. Digest*, pp. 461–464, 1998.

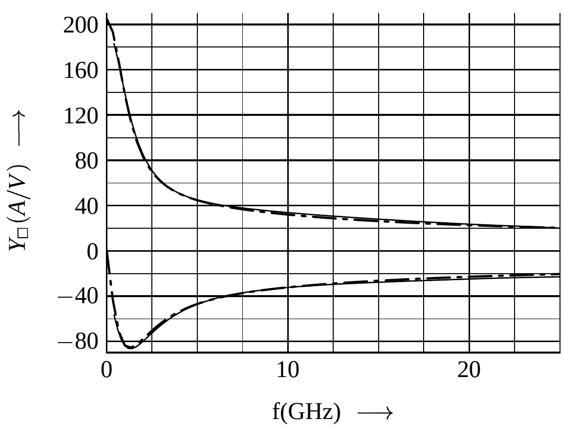

Fig. 5. Real and imaginary Part of the admittance $Y_{\square}$ in dependence of the frequency f. The solid lines represents the approximation obtained from voltage and current FDTD results in a microstrip waveguide's backside metalization (t = 5 μm, σ = 41 MA/Vm), the thin line shows the exact results from the plane skin effect analysis. The FDTD results do not start at a frequency of zero, because a *modulated* Gaussian pulse was used for excitation.

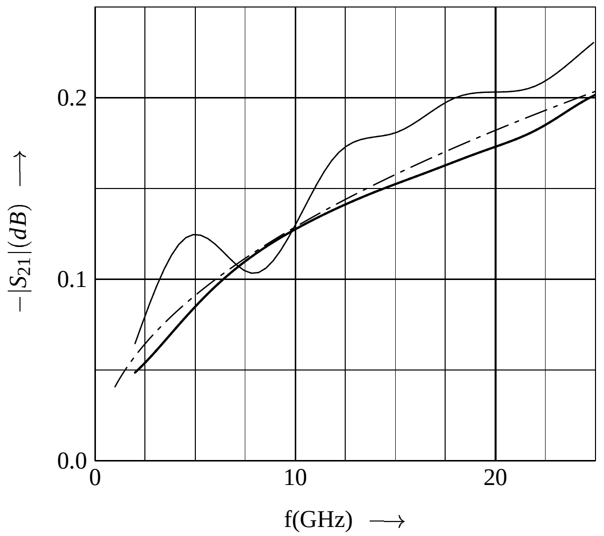

Fig. 6. Attenuation $-|S_{21}|$ of a l = 10 mm long microstrip waveguide (ε_r = 9.8, h = 250 μm, w = 225 μm, t = 5 μm, σ = 41 MA/Vm) in dependence of the frequency f. The thick solid line represents the FDTD results, the thin solid line is measured using open circuits of two different lengths, the other line is obtained using an approximative formula [6]. The FDTD results do not start at a frequency of zero, because a *modulated* Gaussian pulse was used for excitation.

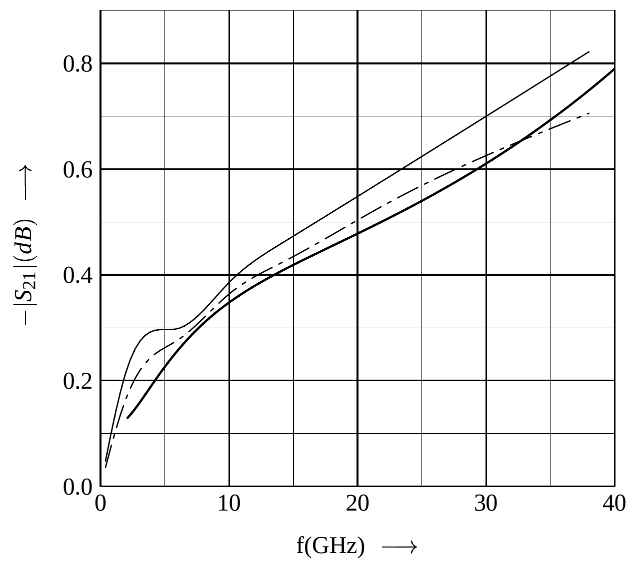

Fig. 7. Attenuation $-|S_{21}|$ of a l = 10 mm long coplanar waveguide (ε_r = 9.8, h = 250 μm, w = 125 μm, d = 225 μm,t = 5 μm, σ = 41 MA/Vm) in dependence of the frequency f. The thick solid line represents the FDTD results, the thin solid line is measured using open circuits of two different lengths, the other line is obtained using a static Finite Difference method in conjunction with an ohmic loss approximation. The FDTD results do not start at a frequency of zero, because a *modulated* Gaussian pulse was used for excitation.